



Optimization of concrete containing wind-turbine wastes following mechanical, environmental and economic indicators

Nerea Hurtado-Alonso^a, Javier Manso-Morato^b, Víctor Revilla-Cuesta^b, Vanesa Ortega-López^b, Marta Skaf^{a,*}

^a Department of Construction, Escuela Politécnica Superior, University of Burgos, c/Villadiego s/n, 09001 Burgos, Spain

^b Department of Civil Engineering, Escuela Politécnica Superior, University of Burgos, c/Villadiego s/n, 09001 Burgos, Spain

ARTICLE INFO

Keywords:

Recycled concrete aggregate
Raw-crushed wind-turbine blade
Concrete
Response surface method
Mechanical performance
Global warming potential
Cost

ABSTRACT

The decommissioning of wind farms produces two primary waste materials: Recycled Concrete Aggregate (RCA) derived from the foundation concrete, and Raw-Crushed Wind-Turbine Blade (RCWTB) obtained through the crushing and sieving of the blades. Incorporating these materials into concrete enhances sustainability and, in some cases, improves mechanical properties while reducing the final environmental impact and cost compared to conventional concrete. A comprehensive characterization of the mechanical properties of concrete mixtures with varying RCA (0–100%) and RCWTB (0–10%) contents was conducted, these mixes being designed with increased water and admixture contents to compensate for the expected loss of workability caused by the addition of these waste materials. A Life-Cycle Assessment (LCA) and cost evaluation were also performed. The optimization of these mixtures was addressed using the Response Surface Method (RSM). The optimization process revealed that intermediate combinations of RCA (50%) and RCWTB (5%) yielded maximum flexural-tensile properties. However, achieving optimal performance proved more challenging when simultaneous optimization included compressive strength and deformability properties, such as modulus of elasticity and Poisson's coefficient. For these properties, the optimal mix incorporated 88% RCA and 0% RCWTB. The RSM analysis demonstrated the feasibility of incorporating both RCA and RCWTB into concrete mixtures, mainly intended to work under bending stresses, but it also highlighted the complexities of achieving optimal performance when all mechanical properties were simultaneously considered. This research underscores the potential for these recycled materials to contribute to more sustainable concrete production while addressing the trade-offs in mechanical performance optimization.

1. Introduction

The construction sector is actively seeking innovative processes to enhance the sustainability of its core operations (Li et al., 2022). This approach involves not only improvements in the execution of infrastructure projects but also in earlier phases, such as material production, and extends to the recycling of materials once the structures in which they are used have reached the end of their useful life (Honic et al., 2021). In this context, the focus is on developing a model based on circular-economy principles (Fort and Černý, 2020), with an emphasis on reducing the use of natural resources through their replacement with different residues rather than solely on recycling waste (Omojola et al., 2022), whether such waste is generated within the construction sector or by other industries. Life-Cycle Assessment (LCA) tools are employed

within this circular-economy framework to evaluate the environmental impacts associated with the production of construction materials (Fenner et al., 2018; Chau et al., 2015), beginning with the extraction of raw materials and continuing through to their final application in building projects. This methodology is vital for the development of materials that incorporate recycled waste from other industries (Luhar and Luhar, 2019), as reintegrating these materials into the production chain mitigates environmental impacts by reducing dependence on natural resources (Habert et al., 2020).

The growing global demand for civil infrastructure leads to a significant consumption of natural resources and the generation of large volumes of waste (Poorisat et al., 2024), resulting from the replacement of obsolete structures with more modern ones (Muresan et al., 2020; Devènes et al., 2023). This issue not only affects the construction industry, where Construction and Demolition Waste (C&DW) exceeds 3.3

* Corresponding author at: Department of Construction, Escuela Politécnica Superior, University of Burgos, c/Villadiego s/n, 09001 Burgos, Spain.

E-mail address: mskaf@ubu.es (M. Skaf).

<https://doi.org/10.1016/j.clema.2025.100317>

Received 17 February 2025; Received in revised form 5 May 2025; Accepted 6 May 2025

Available online 7 May 2025

2772-3976/© 2025 The Authors. Published by Elsevier Ltd. This is an open access article under the CC BY-NC license (<http://creativecommons.org/licenses/by-nc/4.0/>).

Acronym Glossary

LCA	Life-Cycle Assessment
C&DW	Construction and Demolition Waste
RCA	Recycled Concrete Aggregate
RCWTB	Raw-Crushed Wind-Turbine Blade
RSM	Response Surface Method
NA	Natural Aggregates
WA	Water Absorption
SSD	Saturated-Surface-Dry
ANOVA	Analysis Of VAriance
GFRP	Glass Fiber-Reinforced Polymer

billion tons produced annually worldwide (Muñoz Pérez et al., 2024); but also impacts sectors such as renewable energy. Specifically, the wind energy sector is facing a new challenge due to the large number of wind turbines nearing the end of their useful life (Spini and Bettini, 2024). This issue is particularly pressing in Europe, which was among the first regions to adopt wind farms on a large scale (Liu and Barlow, 2017). Previous research has shown that the main waste generated by this industry comes from the decommissioning of these turbines, with projections estimating over 350,000 tons of this waste in Europe alone by 2030 (Spini and Bettini, 2024). Furthermore, the dismantling of these turbines results not only in blade waste but also in Recycled Concrete Aggregate (RCA) obtained from the demolition of their foundations, which can be classified as a type of C&DW.

The scientific literature on the use of RCA as a substitute for natural aggregates in concrete is extensive (Evangelista and de Brito, 2010; Pedro et al., 2017), demonstrating that its use reduces the consumption of natural resources without compromising the mechanical properties or quality of the resulting material following a proper design (Tekle et al., 2021). The main challenge lies in repurposing the decommissioned turbine blades, whose complex composition made up of various materials that are difficult to separate, primarily glass fibers and polymer resins (De et al., 2024), complicates their transformation into reusable materials. Various studies have evaluated processes that try to recover the glass fibers from the blades such as pyrolysis (Zhang et al., 2024) and solvolysis (Xu et al., 2024). A different approach, non-selective crushing of the blades, has shown potential to produce a material designated as Raw-Crushed Wind-Turbine Blade (RCWTB), which constitutes one of the principal waste streams addressed in this research for concrete production. RCWTB is a waste material mainly composed of Glass Fiber-Reinforced Polymer (GFRP) fibers, but that also contains particles of polymers and balsa wood (Revilla-Cuesta et al., 2023), components also found in wind turbine blades (Joustra et al., 2021). GFRP fibers have a rough surface, providing good adhesion to the cementitious matrix of concrete and enhancing its tensile mechanical properties (Xu et al., 2022) through a simple and cost-effective recycling process (Liu et al., 2025). However, the aforementioned weak particles act as low-strength aggregates (Islam et al., 2022), serving as initiation and propagation points for failure under compression loading (Revilla-Cuesta et al., 2024). In this context, the wind energy sector presents an opportunity to investigate the combined use of these two wastes in the production of more sustainable concrete mixtures.

To determine the optimal combination of both waste materials in concrete, it would be necessary to produce a large number of mixtures varying the waste proportions, which would entail a significant consumption of resources, from raw materials to the time required for obtaining results. Optimization tools are therefore essential in identifying the appropriate proportions of concrete main components (Tahir et al., 2023), enabling a more efficient and responsible use of resources. Response Surface Methodology (RSM) is one of the most commonly used optimization methods (Chelladurai et al., 2021), allowing for the

statistical analysis of multiple variables, in this case, two types of waste materials, and their effect on the properties of concrete mixtures. Through this method, it is possible to determine the ideal combinations of materials to maximize critical properties such as compressive and flexural strengths, which are key parameters for the production of structural concrete, while also bearing in mind other aspects such as environmental footprint or production costs (Ulucan, 2024).

The primary objective of this research is to optimize all the mechanical properties of concrete incorporating waste from decommissioned wind farms, specifically RCWTB and RCA, from a holistic perspective. Furthermore, the study aims to identify the optimal incorporation ranges of these wastes to achieve a balance between the structural performance of the concrete and the level of sustainability and cost savings they offer to the concrete industry. After an explanation of the raw materials, mix design, and experimental campaign, an overview of the inputs for the development of the RSM models and optimizations is provided. Then, the study presents an analysis of the mechanical properties of the concrete mixtures, which are subsequently used, along with environmental impact and cost, to conduct modeling and optimization through RSM. The aim of this research is to define the most suitable joint contents of RCA and RCWTB in concrete from a global approach through the application of RSM, in order to advance in a recycling pathway for both wind-turbine wastes, while promoting a cleaner concrete in the construction industry.

2. Materials and methods

2.1. Raw materials

For the concrete mixtures, the following locally available raw materials and wastes were selected.

2.1.1. Cement, water, admixtures and natural aggregates

- An ordinary Portland cement, CEM II/A-L 42.5 R, was used as specified in EN 197-1 (EN-Euronorm, 2020). This cement has a density of 3.05 kg/dm³ and is characterized by limestone addition as clicker replacement ranging from 6% to 20%.
- Regular tap water from the urban supply system at the University of Burgos in Spain was used.
- Two different admixtures supplied by SIKA® were employed. The first one was used to improve the workability of the mixes (Type 1 – 5970) and the second used to reduce the total water requirement (Type 2 – 20HE), while ensuring adequate strength values.
- Four types of aggregates with different fractions were used, whose gradations are depicted in Fig. 1. The aggregates included three fractions of siliceous crushed material: 0/4 mm, 4/12 mm, and 12/22 mm. Their physical properties, as per EN 1097-6 (EN-Euronorm, 2020) were as follows: the 0/4 mm fraction had a Saturated-Surface-Dry (SSD) density of 2.62 kg/dm³ and a 24-hour Water Absorption (WA) of 0.13%; the 4/12 mm fraction had an SSD density of 2.63 kg/dm³ and a 24-hour WA of 0.33%; and the 12/22 mm fraction had an SSD density of 2.60 kg/dm³ and a 24-hour WA of 0.55%. Their fineness moduli (EN 933-1 (EN-Euronorm, 2020) were 3.73, 7.23, and 8.15 units, respectively. Additionally, limestone sand with a fraction of 0/2 mm, having an SSD density of 2.66 kg/dm³, a 24-hour WA of 0.10%, and a fineness modulus of 2.73 units, was also employed.

2.1.2. Recycled Concrete Aggregate (RCA)

4/22 mm size RCA (gradation in Fig. 1) was used as a replacement for the coarse Natural Aggregate (NA) fractions. It was produced by crushing and sieving concrete elements with a compressive strength value of at least 45 MPa, which contained siliceous aggregate. Previous studies have shown that this type of RCA can be effectively used to create structural concrete with satisfactory mechanical performance

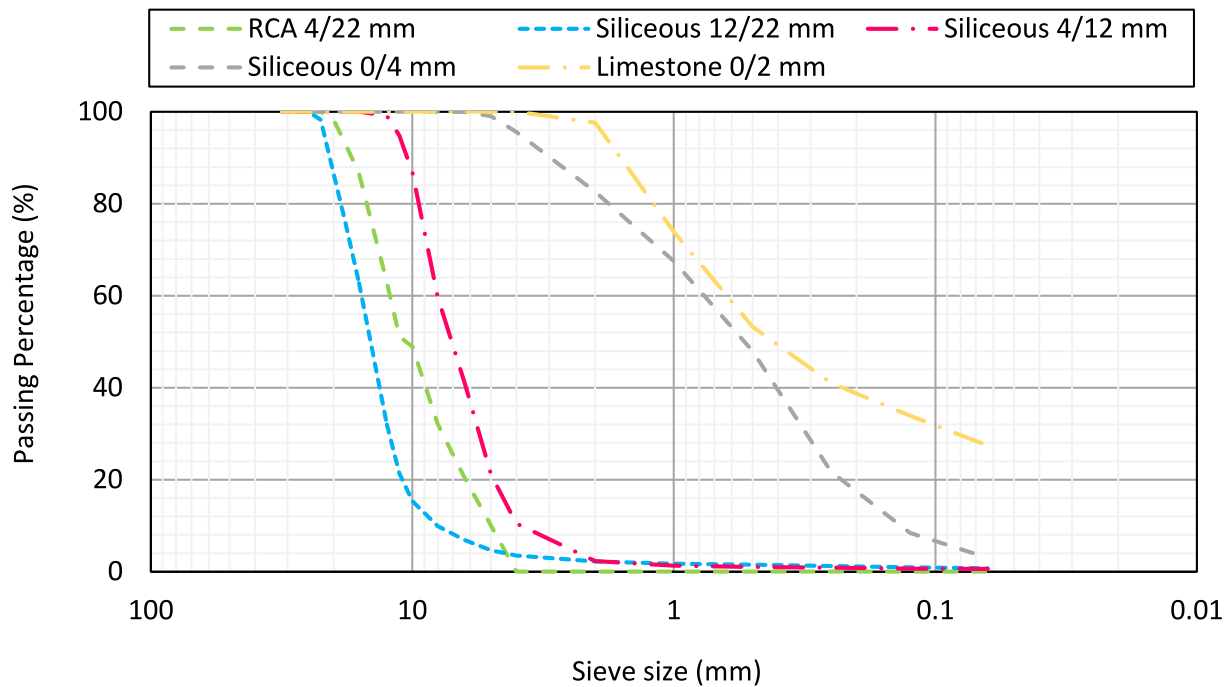


Fig. 1. Aggregates' gradation.

(Pedro et al., 2017).

Compared to NA, the RCA had a lower density (SSD density of 2.44 kg/dm³) and a much higher 24-hour water absorption rate of 6.12%, due to the adhered mortar (Djerbi Tegguer, 2012). Its particle size distribution was continuous, fitting between the 12/22 mm and 4/12 mm fractions of NA (fineness modulus of 7.80 units), and its shape was more irregular, with a rougher surface as shown in Fig. 2. Sourced from a local C&DW treatment facility in Burgos, Spain, this study confirmed that when concrete composition is properly adapted to it, such RCA can be used in concrete for structural applications without negatively affecting

its mechanical properties.

2.1.3. Raw-Crushed Wind-Turbine Blade (RCWTB)

The RCWTB material was obtained through a cutting process of rectangular panels (around 20 cm x 30 cm) sourced from wind turbine blades. Their subsequent non-selective crushing procedure resulted in a raw material primarily composed of GFRP composite fibers, polymers, microfibers, and balsa wood, as depicted in Fig. 3. The physical and mechanical properties of this material have been thoroughly studied in previous investigations by the authors of this paper (Revilla-Cuesta

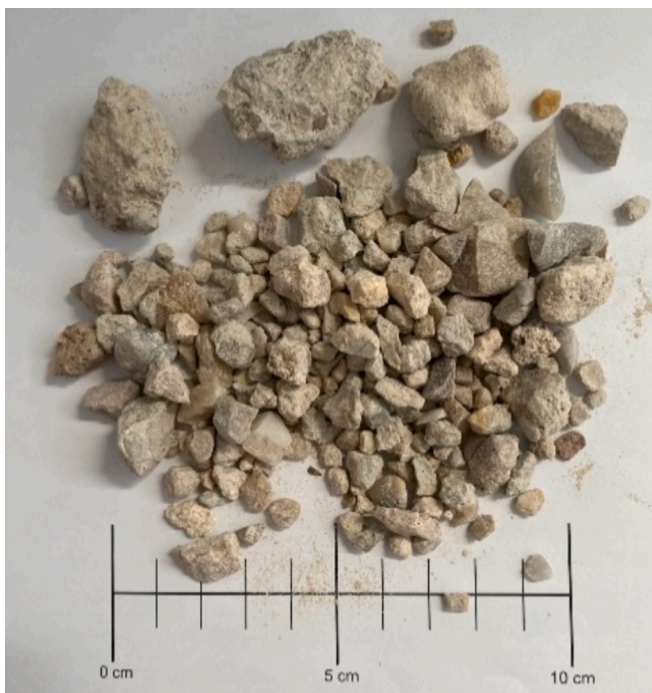


Fig. 2. Coarse recycled concrete aggregate.

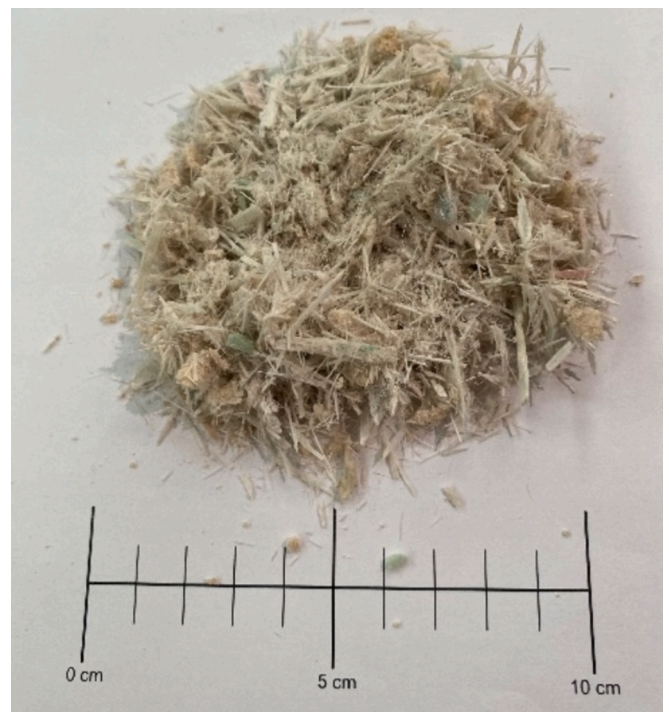


Fig. 3. Raw-crushed wind-turbine blade.

et al., 2023). These studies determined that this composite exhibited a low density of 1.63 kg/dm³ and an apparent density of 246.64 kg/m³. Notably, the fibers constituted 66.8% wt. of the material, whose tensile strength values reached up to 270 MPa. It is worth noting that the composition of the blades may vary, as the proportion of each component depends on factors such as the blade manufacturer or the specific region of the panels from which the cuts are obtained, leading to variations in the material's component distribution.

2.2. Dosage and mix design

The concrete mixes of this research were prepared with varying RCWTB contents (ranging from 0% to 10% of the total aggregate volume), with this material being incorporated as an additional component within the overall composition established in the mix design. Additionally, RCA was used to replace the coarse aggregate fractions, with replacement levels ranging from 0% to 100%. The incorporation ranges for both materials were based on previous research, ensuring adequate workability of the mixes without compromising the strength values of the final concrete (Revilla-Cuesta et al., 2024).

16 mixes with varying waste contents were designed and produced following a central composite design (CCD) (Hossain et al., 2019) with alpha values of ± 0.5 and ± 1 , the optimization design selected for this study, that can be observed in Fig. 4. These alpha values were selected due to their common use in studies applying RSM to concrete, and because they enable a comprehensive coverage of the study space (Hurtado-Alonso et al., 2024). Four of the concrete mixes, which were replicas of the center point of the CCD space corresponding to 5% RCWTB and 50% RCA substitution, were prepared. This approach allowed for a more precise detection of the response curvature in the quadratic regression models, allowing for an accurate evaluation of the performance variability (Li et al., 2020). The contents of both recycled materials were considered as variables to optimize the mechanical, environmental and economic properties of concrete (responses) by the application of RSM models

Regarding the mix proportions of the reference mix (0% waste), the different aggregate fractions were adjusted based on the Fuller's curve. Thus, the aggregates contents were 780 kg/m³, 555 kg/m³, 385 kg/m³, and 280 kg/m³ for the 12/22 mm, 4/12 mm, 0/4 mm and 0/2 mm fractions, respectively. A cement content of 320 kg/m³ was used in accordance with EUROCODE 2 standards (European Committee for Standardization, 2010), along with a water-to-cement ratio of 0.40. Moreover, the two admixtures specified in the materials section of this document were incorporated at 1% of the total cement weight. All the substitutions of conventional raw materials by wastes were conducted with a volume correction based on the densities of the materials

described in previous sections. A workability criterion of a 10 to 15 cm slump (EN 12350-2 (EN-Euronorm, 2020) was set for all the mixes, corresponding to an S3 slump class following EN 206 (EN-Euronorm, 2020), which ensured adequate placement conditions for the concrete regardless of the waste combination used. Thus, empirical adjustments made to the quantities of admixtures and water were performed to maintain the desired workability when the residues were incorporated into the concrete mixes. In particular, the water-to-cement ratio increased by 0.04 for each 50% RCA added to the concrete, while the admixture content was only modified in the mixes with 10% RCWTB, where it increased to 1.3% of the cement mass.

All concrete mixtures were systematically labelled using the prefix *W* to indicate the content of RCWTB, followed by a numeral representing the specific quantity of added material. Similarly, the notation *RCA* was appended, accompanied by a percentage value indicating the level of aggregate substitution. The control or reference mixture, containing no RCWTB and no RCA substitution, was designated as *WORCA0*, representing concrete with 0% incorporation of both recycled materials. The composition of all the concrete mixes is shown in Table 1.

2.3. Experimental campaign

The mixing process was divided into three stages: (1) NA and RCA were mixed with 30% of the water, ensuring that the RCA reached adequate moisture levels to prevent excessive workability loss; (2) RCWTB and cement were added along with the remaining 70% of the water, ensuring proper hydration and distribution of the residue material; (3) both superplasticizers, dissolved in 0.5 L of water, were incorporated during the final mixing stage. Subsequently, the mixtures were ready for casting.

Following the concrete mixing process of each mixture, three specimens were prepared for each hardened-state test, aimed at assessing the mechanical performance of the concrete, with the type and dimensions of the specimens detailed in Table 2. These specimens were cured in a controlled moist chamber at 20 ± 2 °C and $90 \pm 5\%$ relative humidity until the designated testing age. In accordance with EUROCODE-2 (European Committee for Standardization, 2010), the tests were conducted at 28 days, the standardized period for evaluating the mechanical performance of concrete mixes.

2.4. Calculation of global warming potential (GWP) and cost

2.4.1. GWP

The objective of LCA is to evaluate the environmental impact, as well as the resources consumed throughout the life cycle of the concrete, from the environmental burden of the raw materials to the energy

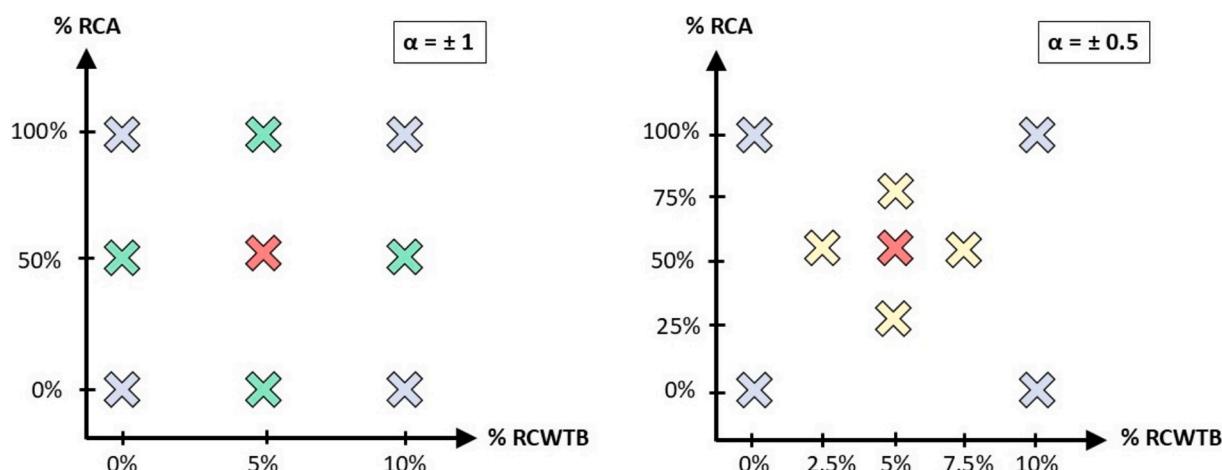


Fig. 4. CCD design for this research.

Table 1
Composition of concrete mixes (kg/m³).

Mix	Cement	Water	20HE	5970	Gravel 12/20 mm	Gravel 4/12 mm	Sand 0/4 mm	Sand 0/2 mm	RCA 4/22 mm	RCWTB
WORCA0	320	128	1.07	2.13	780	555	385	280	0	0
W5RCA0	320	128	1.07	2.13	740	525	365	265	0	62
W10RCA0	320	128	1.33	2.69	700	500	345	250	0	124
W5RCA25	320	135	1.07	2.13	555	395	365	265	295	62
WORCA50	320	142	1.07	2.13	390	280	385	280	625	0
W2.5RCA50	320	142	1.07	2.13	380	270	375	275	605	31
W5RCA50	320	142	1.07	2.13	370	265	365	265	590	62
W7.5RCA50	320	142	1.07	2.13	360	255	355	260	575	93
W10RCA50	320	142	1.41	2.85	350	250	345	250	560	124
W5RCA75	320	149	1.07	2.13	185	130	365	265	890	62
WORCA100	320	156	1.07	2.13	0	0	385	280	1245	0
W5RCA100	320	156	1.07	2.13	0	0	365	265	1185	62
W10RCA100	320	156	1.41	2.85	0	0	345	250	1120	124

Table 2
Concrete testing specifications according to European Standards (EN-Euronorm, 2020) for the mechanical properties evaluated at 28 days.

Test	Standard (EN-Euronorm)	Specimen type
Compressive strength	EN 12390-3	10 × 20-cm cylindrical specimens
Flexural strength	EN 12390-5	7.5 × 7.5 × 27.5-cm prismatic specimens
Splitting tensile strength	EN 12390-6	10 × 20-cm cylindrical specimens
Modulus of elasticity	EN 12390-13	10 × 20-cm cylindrical specimens
Poisson's coefficient	EN 12390-13	10 × 20-cm cylindrical specimens

consumption required for its production. In this case, the LCA focused on the calculation of the Global Warming Potential (GWP) of concrete mixtures containing RCA and RCWTB, following the ISO 14040/44, EN 15804, and EN 15978 standards (EN-Euronorm, 2020). This parameter was assessed over a potential temporal horizon of 100 years, expressed in kilograms of carbon dioxide (kg CO₂-eq) per functional unit. The functional unit was defined as a cubic meter of concrete, which allowed for the comparison of the GWP of the mixtures when varying the contents of RCA and RCWTB. GWP was calculated through the Ecoinvent v3 database (Ecoinvent Centre, 2023) within the SimaPro software version 9 (SimaPro), following the CML-IA Baseline methodology (CML - Department of Industrial Ecology, 2016). Regarding system boundaries, an open-loop cradle-to-gate approach (A1-A3) was employed (Kurda et al., 2018), excluding the previous life cycle stages of both RCA and RCWTB (Nygaard Rasmussen and Birgisdottir, 2016).

To calculate the GWP [kg CO₂-eq/m³] for each mixture, labelled GWP_{WxRCAx}, Equation (1) was applied, based on the amounts of each component (Q_i [kg/m³]). First, the unitary GWP values for each component (GWP_i [kg CO₂-eq/kg]) were determined (Table 3). Then, for transport, packaging, and mixing processes, which remain constant across all mixtures, the corresponding GWP values were estimated based on conventional supply situations in the local concrete industry, and the previously described mixing process. The values for these processes were as follows: transport (TRA = 8.84 kg CO₂-eq/m³), packaging (PAC = 3.28 kg CO₂-eq/m³), and mixing (MIX = 0.48 kg CO₂-eq/m³).

Table 3
GWP values of each component of the concrete mixes.

Raw material	Cement	Water	Plasticizer	Siliceous aggregate	Limestone aggregate	RCA 4/22 mm	RCWTB
GWP (kg CO ₂ -eq)	0.8009	0.0001	0.0066	0.0278	0.0020	0.0000	0.0000

$$GWP_{WxRCAx} = \sum_i (GWP_i \times Q_i) + TRA + PAC + MIX \tag{1}$$

2.4.2. Cost

An economic analysis was also conducted regarding the cost of each concrete mix, considering only the unitary costs of its components. Other factors, such as transportation cost of the mixtures, were assumed to remain constant across the different concrete mixtures analyzed. First, to calculate the cost of each mixture per cubic meter (Cost_{WxRCAx} [€/m³]), it was necessary to determine the unitary cost of each component (Unitary cost_i [€/kg]).

- In the case of cement, the value was obtained from an official price database in Spain (Government of Extremadura, 2024).
- For the different fractions of natural aggregates and RCA (recycled concrete aggregates), the prices were provided by private suppliers.
- The admixtures were purchased from the commercial brand SIKA®, which provided the unitary price for both superplasticizers.
- In the case of RCWTB material, the value was determined in collaboration with the companies involved in the recycling process, taking into account preliminary estimates of energy consumption and transportation costs associated with its production.

All unitary prices are presented in Table 4. It is worth noting that the unitary costs of the two types of waste materials used in the mixtures are lower than those derived from natural resources, which provides a cost advantage over the production of conventional mixtures. Once the unitary costs were determined, the quantity of each component (Q_i [kg/m³]) was multiplied by its corresponding value, and the total sum yielded the final cost of each mixture per cubic meter (Equation (2)).

$$Cost_{WxRCAx} = \sum_i (Unitary\ cost_i \times Q_i) \tag{2}$$

2.5. Model development

The optimization model through RSM was developed using Design Expert version 13.0.5 software, applying a CCD, which is widely used due to its efficiency, reducing the number of experimental runs needed to explore the model's search space (Alqadi et al., 2012). In this case, two key factors, RCWTB and RCA, were considered, both expressed as percentages and defined previously in this document in Section 2.2.

Table 4
Unitary cost of raw materials.

Raw material	Cement	Water	20HE	5970	Gravel 12/20 mm	Gravel 4/12 mm	Sand 0/4 mm	Sand 0/2 mm	RCA 4/22 mm	RCWTB
Cost (€/kg)	0.1112	0.0012	5.0140	5.0880	0.0110	0.0110	0.0103	0.0103	0.0038	0.0052

These factors were varied at five levels: -1 , -0.5 , 0 , $+0.5$, and $+1$, where 0 represents the central level, while -1 and $+1$ indicate the extremes of the experimental range. The objective of this design was to optimize all mechanical properties of the concrete mixes (compressive strength, flexural strength, splitting tensile strength, modulus of elasticity and Poisson’s coefficient) along with GWP, which measures environmental impact and finally, the cost of each mixture. All these concrete properties acted as responses in the model, strictly considering their experimental average values.

CCD with $k = 2$ factors and 5 levels (alpha values of ± 0.5 and ± 1) enabled a comprehensive evaluation of linear, quadratic, and interaction effects between RCWTB and RCA. In order to determine the most appropriate mathematical model, whether linear (Equation (3) or quadratic (Equation (4)), an ANalysis Of VAriance (ANOVA) was conducted for each response. This analysis allowed the identification of the best-fitting model to describe the relationships between the factors and the responses, where the following key metrics were evaluated: p-value of the model, lack of fit and R^2 coefficient (coefficient of determination). The best-fitting models were used to perform the optimization, whose details are explained in the following subsection.

$$Y = \beta_0 + \sum_{i=1}^k \beta_i X_i + \epsilon_0, \tag{3}$$

$$Y = \beta_0 + \sum_{i=1}^k \beta_i X_i + \sum_{i=1}^k \beta_{ii} X_i^2 + \sum_{i=1}^k \sum_{j>1}^k \beta_{ij} X_i X_j + \epsilon_0, \tag{4}$$

The whole process followed for the optimization using RSM is shown in Fig. 5, which schematically summarizes the different steps involved in this procedure.

2.6. Case studies

Based on the characteristics defined in Section 2.5 for the development of the optimization models, the RSM allows for two types of optimization processes: graphical optimization and numerical optimization. In this section, various scenarios are defined for the application of concrete mixtures incorporating RCA and RCWTB, where different mechanical properties and characteristics are optimized. Six case studies are presented for graphical optimization, and three scenarios are presented for numerical optimization.

The details of each case related to **graphical optimization** are as follows:

- Case 1: In this case, compressive strength, modulus of elasticity and Poisson’s coefficient are optimized. The target value for compressive strength must exceed 45 MPa, and the modulus of elasticity should surpass 40 MPa. The Poisson’s coefficient is required to be within the range of 0.160 to 0.190, being in accordance with the experimental results. These criteria align with the requirements for high-strength concrete or prestressed concrete elements suitable for structural applications according to the European EUROCODE-2 (European Committee for Standardization, 2010) or the Spanish Structural Code (Gobierno de España, 2021).
- Case 2: To achieve conventional concrete, meeting structural requirements without demanding high mechanical performance (European Committee for Standardization, 2010), the defined compressive strength should range between 26 and 40 MPa, the modulus of elasticity should range between 30 and 35 MPa, and the Poisson’s coefficient should fall within the range of experimentally obtained values. These characteristics make this case suitable for a variety of applications, such as pavements, retaining walls or non-critical foundations (Rambabu et al., 2022).
- Case 3: This case applies to elements requiring high flexural strength (Yao et al., 2022). The properties optimized in this scenario include flexural strength with a lower limit of 5.5 MPa and a splitting tensile strength exceeding 3.5 MPa. Some potential application typologies for this case could include long-span beams (European Committee for Standardization, 2010).
- Case 4: This case focuses on the development of conventional concrete optimized to achieve a flexural strength within the range of 4.5 to 5.5 MPa and a splitting tensile strength between 3.0 and 3.5 MPa (Yao et al., 2022). Such properties make this material particularly suitable for applications in structural elements, with notable examples including pavements (Rambabu et al., 2022).
- Case 5: This case results from the combination of Case 1 and Case 3, representing high-performance concrete with optimization of all mechanical properties, following the standard values defined in the EUROCODE-2 (European Committee for Standardization, 2010). The target values are as follows: compressive strength exceeding 45 MPa, modulus of elasticity above 40 MPa, Poisson’s coefficient between 0.160 and 0.190 within the experimental interval of results, flexural strength above 5.5 MPa, and splitting tensile strength above 3.5 MPa.
- Case 6: Last case focuses on conventional concrete (European Committee for Standardization, 2010) with optimization of all its mechanical properties (combination of Case 2 and Case 4). The range of

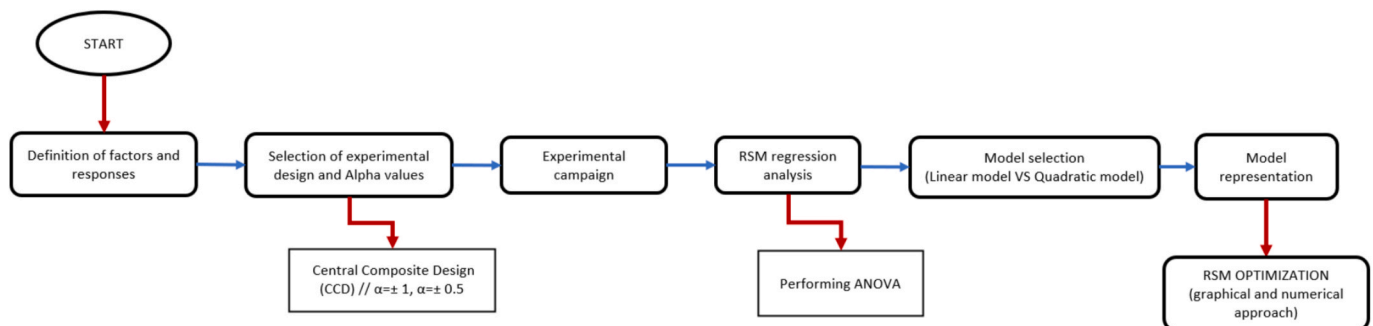


Fig. 5. Flowchart of the RSM optimization process.

values is as follows: compressive strength between 26 – 40 MPa, modulus of elasticity between 30 – 35 MPa, Poisson’s coefficient within the normal range, flexural strength between 4.5 – 5.5 MPa, and splitting tensile strength between 3 – 3.5 MPa.

The upper and lower limit values established for each property in the various cases are summarized in Table 5. Furthermore, it is important to note that for all the cases defined above, both GWP and the cost of the mixtures are considered to be within the normal range.

From the perspective of numerical optimization, the three scenarios defined in Table 6 were studied, where the methodology for maximizing, minimizing, or keeping each evaluated property within a specified range is as indicated in the table. Scenario 1 intended to maximize compressive performance, Scenario 2 the bending-tensile behavior, and Scenario 3 both dimensions of concrete performance simultaneously.

3. Results and discussion: Properties

3.1. Mechanical properties analysis

The mechanical properties evaluated in the experimental campaign are presented in Table 7 along with their standard deviations. The standard deviations showed variation within appropriate limits for the application of RSM (Hurtado-Alonso et al., 2024). The following paragraphs analyze these values and explain the behavior of each mixture.

In terms of compressive strength, all mixtures achieved a minimum value of 25 MPa, qualifying as structural concrete (European Committee for Standardization, 2010), including the mixture with the highest content of both waste materials, W1ORCA100 (26.84 MPa). Increasing the RCWTB content generally led to a reduction in strength values, which is attributed to the reduced adhesion in the Interfacial Transition Zones (ITZ) between the polymer and wood particles to the cementitious matrix (Islam et al., 2022). However, the effect of this loss of adhesion was less significant, as it was mitigated by a stitching effect generated by the fibers at the failure point (Xu et al., 2022), with final strength reductions ranging between only 13% and 17%. On the other hand, when the replacement of NA with RCA was increased, the losses were minimal and even improved at certain points. Both the good quality of the parent concrete (Padmini et al., 2009) and the adjusted increase of the water/cement ratio when adding RCA (Pedro et al., 2017) explain why strength values did not decrease significantly when increasing the RCA content.

The flexural strength of the concrete mixtures was evaluated, with findings indicating substantial enhancements with the addition of RCWTB, especially in conjunction with a 50% replacement of RCA. The observed increase in flexural strength was 0.82 MPa between the WORCA0 and W1ORCA50 mixtures, with overall improvements in flexural strength of 15% when RCWTB was incorporated. The presence of fibers in RCWTB positively impacted flexural behavior by reinforcing

crack-bridging effects, leading to enhanced strength values, particularly in the W1ORCA50 mixture. These results indicate that the synergistic use of RCWTB with intermediate RCA levels, leveraging the mechanical properties contributed by the strength of the parent concrete (Padmini et al., 2009), holds promise for improving the flexural properties of concrete mixtures that incorporate recycled materials.

To comprehensively assess the bending-tensile behavior, splitting tensile strength tests were also conducted, the characteristics values being considered. In general, high RCA contents were associated with a decrease in tensile strength. This was attributed to increased amounts of adhered mortar from the RCA, which created ITZ with higher porosity (Memon et al., 2022), that promoted aggregate detachment within the cementitious matrix, resulting in lower tensile strength values. The porosity of the cementitious matrix may also have increased due to the higher water and admixture contents when adding both wastes, which also contributed to the weakening of the ITZ (Revilla-Cuesta et al., 2024). However, the incorporation of RCWTB, which contains a high proportion of GFRP-composite fibers that bridged the concrete matrix (Haider et al., 2021) even led to improvements over the reference mixture, as demonstrated by the W1ORCA50 mixture, which exhibited a tensile strength value of 3.79 MPa. Once again, the best RCWTB performance was found when combined with 50% RCA.

With respect to the properties analyzed to characterize deformability, both RCWTB and RCA exhibited comparable effects in both the load-parallel and load-perpendicular directions, reflected in the modulus of elasticity and Poisson’s coefficient, respectively. At maximum replacement levels of both residues, a notable reduction in the modulus of elasticity of 47% was observed. This reduction is partly attributed to the increased proportion of balsa wood and polymer particles in higher RCWTB contents, materials that are considerably more deformable than NA and also RCA (Da Silva and Kyriakides, 2007). The increase in the amount of water and admixtures when adding RCA and RCWTB could also weaken the cementitious matrix, thus favoring such performance (Revilla-Cuesta et al., 2023). Both aspects simultaneously resulted in a more pronounced decrease compared to mixtures where only RCA is used. For Poisson’s coefficient, the trend suggested that lower RCWTB contents improved stiffness and reduced lateral deformability in these mixtures, particularly with moderate RCA proportions, as seen in the W2.5RCA50 mixture. Finally, at maximum replacement levels, the observed increase in deformability for mixtures with a 10% RCWTB content showed similar trends when combined with high RCA percentages.

3.2. Life-cycle assessment

Fig. 6 illustrates the graphical representation of the LCA results, specifically focusing on the calculation of GWP values expressed in kg CO₂-eq/m³, as described comprehensively in the methodology in Section 2.4.1.

The results indicate that the reference concrete mix exhibited a GWP value of approximately 286 kg CO₂-eq/m³. However, as RCWTB was progressively introduced and NA was replaced with RCA, the GWP values varied between 280 and 253 kg CO₂-eq/m³. These findings suggest a notable improvement in the environmental performance of the concrete mixes with the incorporation of materials derived from decommissioned wind turbine blades. It is worth noting that all concrete mixes maintained the original cement content of the reference mix. On the other hand, increasing RCWTB amounts did not always lead to GWP reductions. In fact, the addition of RCWTB sometimes led to an increase of GWP values when using the same level of RCA substitution. For instance, the mixes WORCA50, W2.5RCA50, and W1ORCA50 exhibited GWP values of 272.88, 262.27 and 269.87 kg CO₂-eq/m³, respectively. Such increases in GWP when adding RCWTB are attributed to the increase in the water and admixtures contents when incorporating this waste into concrete, which was required to ensure that all the mixes achieved acceptable levels of workability when adding high RCWTB

Table 5
Boundary values of properties for the cases associated with graphical optimization.

Property	Case 1	Case 2	Case 3	Case 4	Case 5	Case 6
Compressive strength (MPa)	$x \geq 45$	$26 \geq x \geq 40$	–	–	$x \geq 40$	$26 \geq x \geq 40$
Flexural strength (MPa)	–	–	$x \geq 5.5$	$4.5 \geq x \geq 5.5$	$x \geq 5.5$	$4.5 \geq x \geq 5.5$
Splitting tensile strength (MPa)	–	–	$x \geq 3.5$	$3.0 \geq x \geq 3.5$	$x \geq 3.5$	$3.0 \geq x \geq 3.5$
Modulus of elasticity (GPa)	$x \geq 40$	$30 \geq x \geq 35$	–	–	$x \geq 35$	$30 \geq x \geq 35$
Poisson’s coefficient	$0.16 \geq x \geq 0.19$	In range	–	–	$0.16 \geq x \geq 0.19$	In range

Table 6
Optimization criteria for each property evaluated in the numerical optimization.

Scenario	Compressive strength	Flexural strength	Splitting tensile strength	Modulus of elasticity	Poisson's coefficient	GWP	Cost
Scenario 1	Maximize	none	none	Maximize	In range	Minimize	Minimize
Scenario 2	none	Maximize	Maximize	none	none	Minimize	Minimize
Scenario 3	Maximize	Maximize	Maximize	Maximize	In range	Minimize	Minimize

Table 7
Full mechanical characterization of concrete mixtures with RCWTB and RCA content.

Mixture ID	RCWTB (%)	RCA (%)	Compressive strength [MPa]	Flexural strength [MPa]	Splitting tensile strength [MPa]	Modulus of elasticity [GPa]	Poisson's coefficient
W0RCA0	0	0	47.2 ± 3.4	5.59 ± 0.52	3.77 ± 0.22	45.3 ± 0.9	0.167 ± 0.015
W5RCA0	5	0	40.9 ± 4.0	5.91 ± 0.56	3.68 ± 0.36	37.9 ± 1.8	0.161 ± 0.008
W10RCA0	10	0	39.3 ± 2.8	5.44 ± 0.35	3.64 ± 0.25	33.8 ± 0.7	0.183 ± 0.011
W5RCA25	5	25	45.0 ± 1.8	5.44 ± 0.45	3.59 ± 0.36	38.3 ± 1.7	0.188 ± 0.043
W0RCA50	0	50	48.2 ± 1.6	5.64 ± 0.56	3.50 ± 0.25	40.0 ± 1.8	0.164 ± 0.013
W2.5RCA50	2.5	50	39.5 ± 1.0	5.42 ± 0.50	3.29 ± 0.09	35.7 ± 1.4	0.151 ± 0.005
W5RCA50	5	50	41.9 ± 1.7	5.28 ± 0.28	3.53 ± 0.31	34.1 ± 1.6	0.157 ± 0.011
W7.5RCA50	7.5	50	38.9 ± 1.9	5.26 ± 0.07	3.05 ± 0.29	32.1 ± 1.2	0.183 ± 0.022
W10RCA50	10	50	42.5 ± 0.8	6.41 ± 0.34	3.79 ± 0.24	28.6 ± 0.4	0.192 ± 0.030
W5RCA75	5	75	36.7 ± 1.8	5.51 ± 0.21	3.45 ± 0.08	32.6 ± 1.0	0.165 ± 0.010
W0RCA100	0	100	43.7 ± 1.3	4.46 ± 0.58	3.37 ± 0.50	32.8 ± 0.6	0.184 ± 0.028
W5RCA100	5	100	36.7 ± 3.6	4.76 ± 0.13	2.88 ± 0.37	27.9 ± 0.4	0.164 ± 0.015
W10RCA100	10	100	26.8 ± 2.1	4.88 ± 0.28	2.60 ± 0.08	23.7 ± 0.7	0.182 ± 0.016

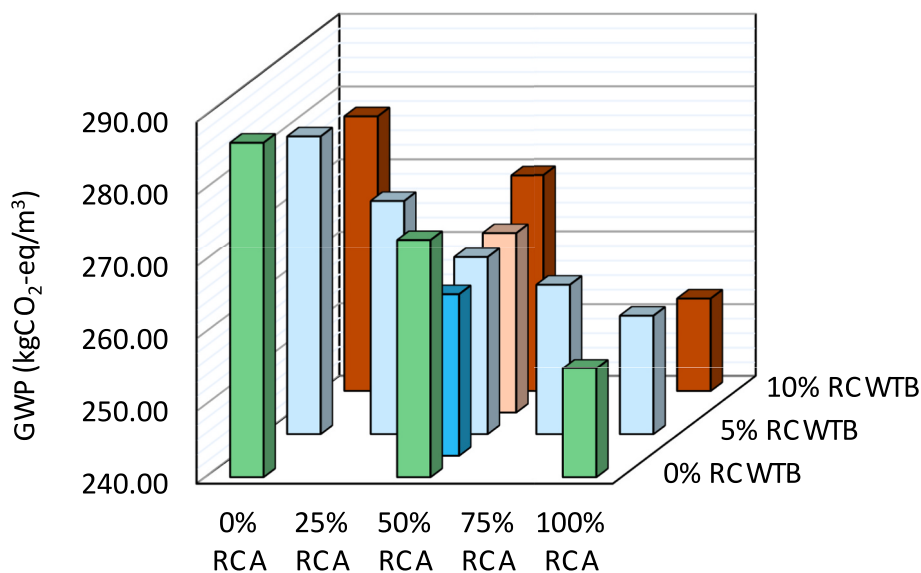


Fig. 6. Effect of RCWTB and RCA on the GWP of the concrete mixtures.

amounts.

As an overall conclusion, it can be stated that the integration of any RCA content and up to 7.5% RCWTB into concrete mixes significantly enhances their sustainability mainly by reducing the reliance on raw materials sourced from natural resources and providing an effective end-of-life application for waste materials that would otherwise be accumulated in landfills. However, the use of high RCWTB contents (10%) results in a potential increase of the environmental impact due to the adjustment of the amounts of water and admixtures.

3.3. Cost evaluation

The costs of the concrete mixes are presented in Fig. 7, calculated in accordance with the methodology outlined in Section 2.4.2. As the use of waste-derived materials increased, the reliance on natural raw materials decreased, resulting in production costs for the mixes being lower than those of the reference mix (73.41 €/m³) in almost all the mixes

incorporating wastes. Cost reductions of up to 9% were steadily observed with every 50% substitution of RCA. This trend, however, was less consistent with RCWTB, as its addition sometimes led to higher costs of the concrete mix. In fact, the mix W10RCA0 exhibited a higher cost than the reference mix (74.22 €/m³). This increase was attributed to the greater quantities of admixtures required for these dosages, which consequently raised the final production costs. Therefore, while RCWTB incorporation generally contributed to cost reductions, some exceptions were noted, highlighting the influence of specific adjustments or processing requirements associated with the production of concrete with this material.

4. Optimization by response surface method: Modeling

For the selection of models through ANOVA calculations, the experimental mean values of each property were strictly used, with the exception of the central point corresponding to the W5RCA50 mixture.

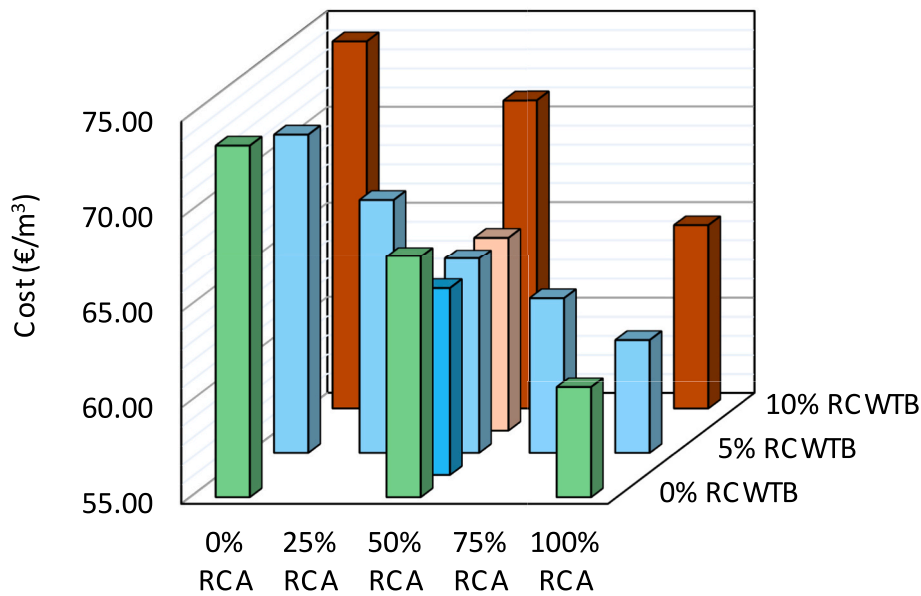


Fig. 7. Cost for each combination of RCWTB and RCA in the concrete mixtures.

In this case, as it represented the replication point, four experimental average values were obtained for each evaluated property. Table 8 and Table 9 depict the values of the metrics considered to evaluate the fitting quality of both linear and quadratic models for alpha values of ±1 and ±0.5, respectively.

After a thorough evaluation of the ANOVA results, the following key conclusions have been drawn regarding the optimization models for each evaluated property, considering a significance level of 10%:

- For compressive strength, the quadratic model showed a better fit with a higher R² (0.8212 for alpha = ±1) across both alpha values, although both the linear and quadratic models were found to be statistically significant.
- In the case of flexural strength, neither model was clearly superior; however, the quadratic model presented a slightly better fit in terms of R², even though the p-values were not always significant.
- For splitting tensile strength, the quadratic model presented a higher R² and was always significant, indicating a better overall fit.
- Regarding the modulus of elasticity, both models exhibited very high R² values, but the quadratic model offered a marginally better fit. In contrast, for Poisson’s coefficient, neither model provided a good fit, as the p-values were not significant and the R² values were low (with a maximum of 0.6796).
- For the environmental impact (GWP), the quadratic model was preferable across both alpha configurations, due to its higher R².
- Finally, for cost, while both models were statistically significant, the quadratic model provided a superior fit in terms of R².

In summary, the quadratic model was globally selected as the

optimal choice for all responses, as it generally provided a better fit for explaining the variability in the results obtained and the lack of fit was never significant. This uniformity allows stable analysis and more accurate conclusions to be reached.

Once the quadratic model was chosen, the optimal value of α was determined for each case:

- Properties such as compressive strength, modulus of elasticity, and Poisson’s coefficient, related to the compression behavior of concrete, exhibited the best R² fit values with α = ±1, achieving R² values of 0.8218, 0.9823, and 0.6796, respectively. Fig. 8 illustrates the response surfaces obtained for each case, highlighting the influence of RCWTB and RCA on these properties (Fig. 8a, Fig. 8d, and Fig. 8e).
- An alpha value of ±0.5 was identified as the most appropriate for properties such as flexural strength, splitting tensile strength, GWP, and cost, as it resulted in a superior fit compared to α = ±1. The 3D response surface plots for these properties are depicted in Fig. 8b, Fig. 8c, Fig. 8f, and Fig. 8g, respectively.

In the first set of optimized properties (alpha = ±1), the 3D and contour plots and their corresponding curvatures demonstrated that each response exhibited a distinct non-linear behavior as both factors (waste contents) increased. Notably, certain responses displayed more pronounced curvatures compared to others, highlighting differences in sensitivity to the factors. It is worth emphasizing that the regions of the plots shaded in colors closer to red represent the specific combinations of RCWTB and RCA that result in the maximum values for each property.

Table 8
ANOVA results for alpha=±1.

Responses (Alpha=±1)	Linear model			Quadratic model		
	P-value	Lack of fit (model)	R ² value	P-value	Residual (Lack of fit)	R ²
Compressive strength [MPa]	0.0141	0.4505	0.6121	0.0299	0.6358	0.8218
Flexural strength [MPa]	0.0521	0.1546	0.4814	0.0953	0.1334	0.6778
Splitting tensile strength [MPa]	0.0232	0.4715	0.5667	0.0703	0.5214	0.7562
Modulus of elasticity [GPa]	< 0.0001	0.8012	0.9728	< 0.0001	0.8469	0.9823
Poisson’s coefficient [-]	0.5054	0.4746	0.1407	0.1433	0.8417	0.6796
GWP [kg CO ₂ -eq]	< 0.0001	0.3646	0.9084	0.0012	0.3344	0.9422
Cost [€/kg]	0.0004	0.0267	0.8273	0.0001	0.1704	0.9739

Table 9
ANOVA results for $\alpha = \pm 0.5$.

Responses ($\alpha = \pm 0.5$)	Linear model			Quadratic model		
	P-value	Lack of fit (model)	R ² value	P-value	Residual (Lack of fit)	R ²
Compressive strength [MPa]	0.0045	0.6502	0.6991	0.0436	0.6119	0.7958
Flexural strength [MPa]	0.0456	0.5089	0.4966	0.1288	0.5143	0.6927
Splitting tensile strength [MPa]	0.0200	0.6130	0.5808	0.0521	0.7718	0.7820
Modulus of elasticity [GPa]	< 0.0001	0.7213	0.9581	0.0001	0.7777	0.9741
Poisson's coefficient [-]	0.7085	0.3905	0.0737	0.5961	0.3452	0.3953
GWP [kg CO ₂ -eq]	< 0.0001	0.4803	0.9076	0.0005	0.6706	0.9570
Cost [€/kg]	0.0003	0.0576	0.8295	< 0.0001	0.8475	0.9874

- For compressive strength (Fig. 8a and Fig. 9a), the maximum value was achieved with RCWTB contents below 3% and moderate levels of NA replacement by RCA. The surface curvature for this optimization was slightly concave, indicating an optimal range for both factors where compressive strength is maximized. Furthermore, the elevated compressive strength values, represented by the warmer colors, were observed at moderate levels of both RCWTB and RCA. This suggests that achieving a balance between the two waste materials is crucial for optimizing this property.
- In contrast, the modulus of elasticity (Fig. 8d and Fig. 9d) presented a less pronounced surface curvature, indicating smoother changes. This implies that the addition of RCWTB and RCA caused less critical changes in this property, as the resulting value exhibited a more linear trend. Furthermore, the contour lines projected onto the horizontal plane were parallel, indicating minimal interaction between the two materials regarding their influence on the modulus of elasticity.
- Finally, the response surface for optimizing Poisson's coefficient (Fig. 8e and Fig. 9e) exhibited an upward-facing concave curvature. This suggests that the lowest Poisson's coefficient values were observed at intermediate combinations of RCWTB and RCA. Deviations from these intermediate combinations resulted in significant increases in Poisson's coefficient, particularly at the extremes.

For the remaining optimized properties, those modelled with an alpha value of ± 0.5 , the 3D and contour representations showed similar results in both sets. This was the case for the two properties responsible for defining the bending-tensile behavior, where the curvatures of both surfaces were very similar. Conversely, in the case of GWP and cost, both reached their minimum values for similar waste combinations. Each resulting model is briefly analyzed below:

- The flexural strength (Fig. 8b and Fig. 9b) response surface exhibited a downward-facing concave curvature, with reddish tones concentrated along the RCWTB axis. This indicates that the maximum value for this property was achieved near intermediate levels of RCWTB, combined with RCA contents in the range of 0–20%. However, this analysis disregards the implicit variability of this property and the trend parallelism with the fiber content typical in fiber-reinforced concrete (Yao et al., 2022; Ahmed and Lim, 2021).
- For splitting tensile strength (Fig. 8c and Fig. 9c), two distinct regions along the RCA axis yielded optimal combinations: one near 0% RCA and the other near 100%. In both cases, the maximum values for this property were observed with RCWTB contents around 5%.
- Both non-mechanical properties related to environmental and economic factors, GWP (Fig. 8f and Fig. 9f) and cost (Fig. 8g and Fig. 9g), displayed similar response surfaces concerning the influence of both wastes. These surfaces exhibited low curvature but steep slopes along the RCA axis, indicating that variations in these properties reached their maximum values when increasing the content of this alternative aggregate. The addition of RCWTB was not so relevant, due to the necessary water and admixture adjustment. This explains why the minimum GWP values were observed at the highest possible

replacement levels of NA with RCA. Correspondingly, the production costs relative to conventional concrete were also lower for these same combinations.

5. Optimization by response surface method: Outputs

Once each property was individually optimized to determine the most suitable alpha, the corresponding optimizations were conducted for the case studies outlined in Section 2.6. To achieve unified multi-objective optimization, the models obtained with $\alpha = \pm 1$ were applied across all properties, as the variations in values obtained from the ANOVA were negligible in terms of overall desirability. This section presents the graphical results (Fig. 10) and numerical results (Fig. 11) of the optimization process for each case and analyzes the influence of both waste materials on the various concrete types.

5.1. Graphical optimization

To evaluate the effectiveness of the graphical optimization process, it is essential to recognize that each property is represented by an area enclosed by contour curves. The overlap of these areas defines a yellow-shaded region, which represents the optimal zone where all conditions established for the optimization are simultaneously satisfied. This region corresponds to specific combinations of the independent variables (RCWTB and RCA). The contour lines themselves delineate the surfaces at which the target values for individual properties are achieved.

5.1.1. Case study 1

The 2D graph (Fig. 10.1) identifies the optimal region for this concrete type, which resulted in a notably compact area, emphasizing the challenge of simultaneously meeting target values for multiple properties. Achieving this required highly precise adjustments in the proportions of RCWTB and RCA. Outside this optimal region, which spans approximately 0–1% RCWTB and 0–50% RCA, the individual property targets could be achieved only independently. For example, while the desired modulus of elasticity was reached in certain areas, the target compressive strength was not met, reflecting a trade-off between mechanical properties like compressive strength and deformability-related ones.

The limited span of the optimal region, approximately 0–45% along the RCA axis and 0–1.5% along the RCWTB axis, highlights the sensitivity of concrete compression-related properties to small variations in mix proportions. Balancing compressive strength, elastic modulus, and Poisson's coefficient thus proved particularly challenging, underscoring the complexity of designing mixes to achieve multi-objective performance criteria.

5.1.2. Case study 2

For alternative target values but the properties optimized as in Case Study 1, the resulting feasible region differed markedly, as illustrated in Fig. 10.2. This constitutes Case Study 2. Similar to the previous case, the analysis of the optimized region reveals a slender, elongated band, emphasizing the stringent constraints in achieving both target properties

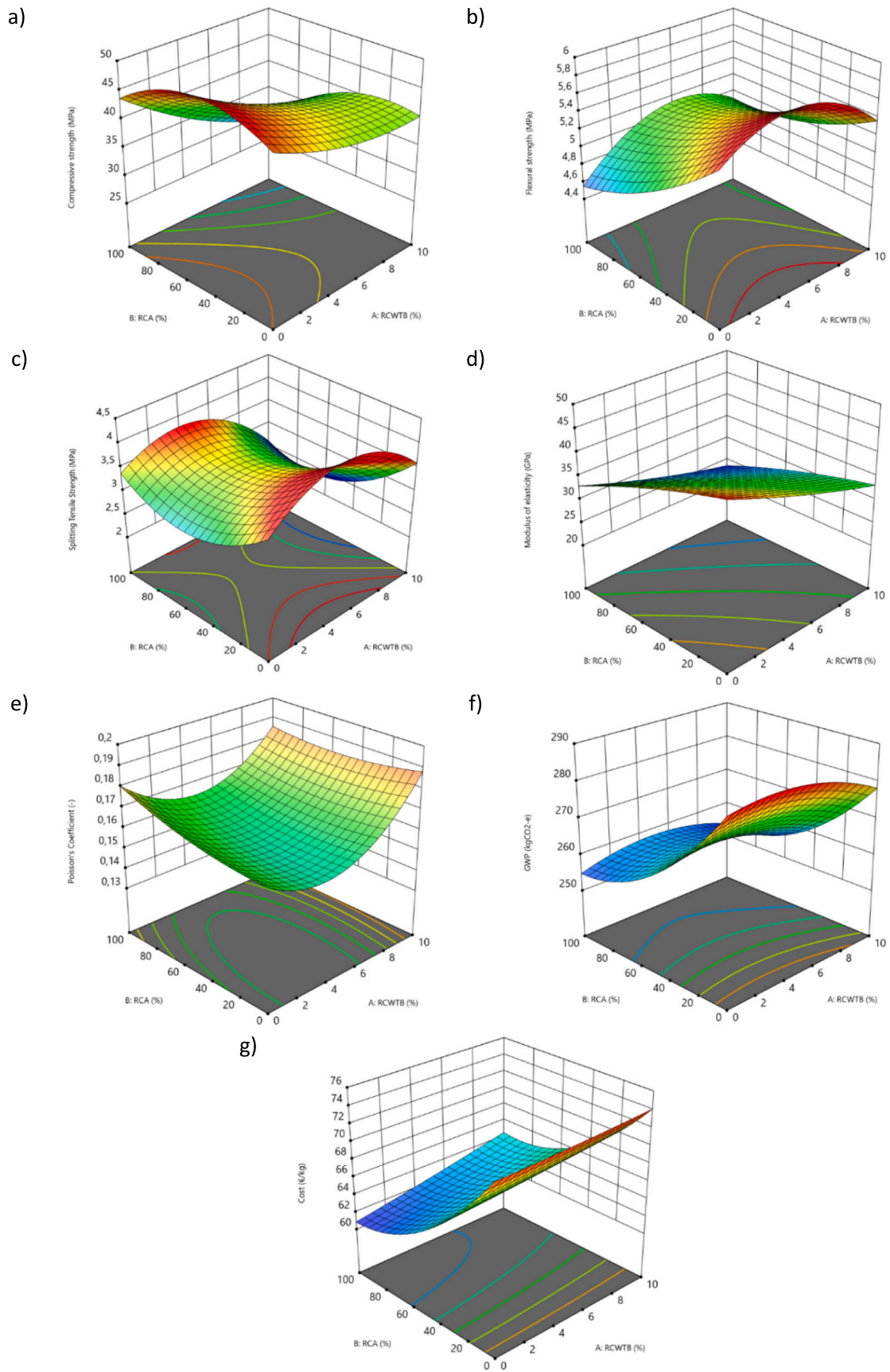


Fig. 8. 3D surfaces of the optimum quadratic models: (a) compressive strength; (b) flexural strength; (c) splitting tensile strength; (d) modulus of elasticity; (e) Poisson's coefficient; (f) GWP; (g) cost.

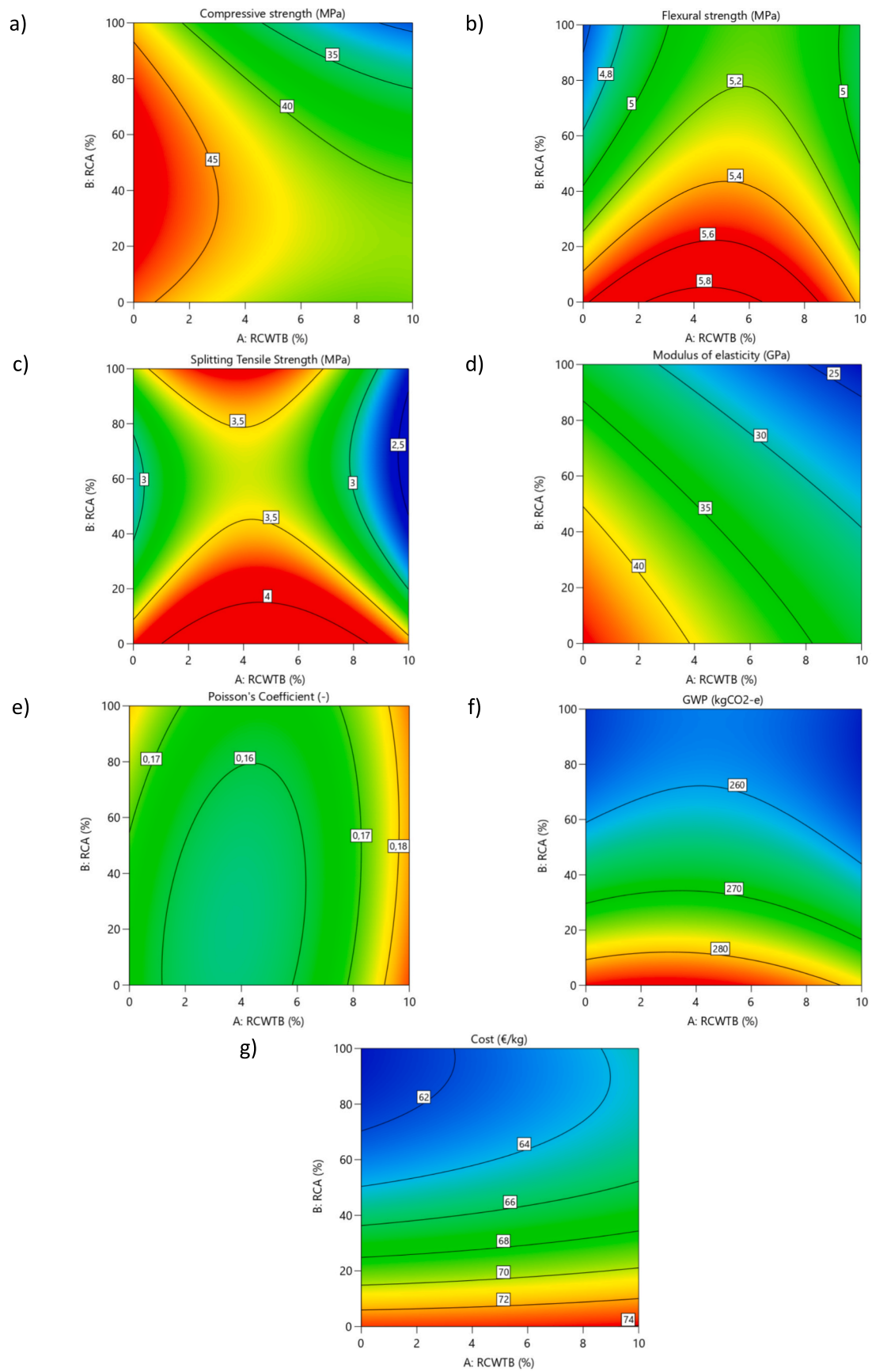


Fig. 9. Contour plots of the optimum quadratic models: (a) compressive strength; (b) flexural strength; (c) splitting tensile strength; (d) modulus of elasticity; (e) Poisson's coefficient; (f) GWP; (g) cost.

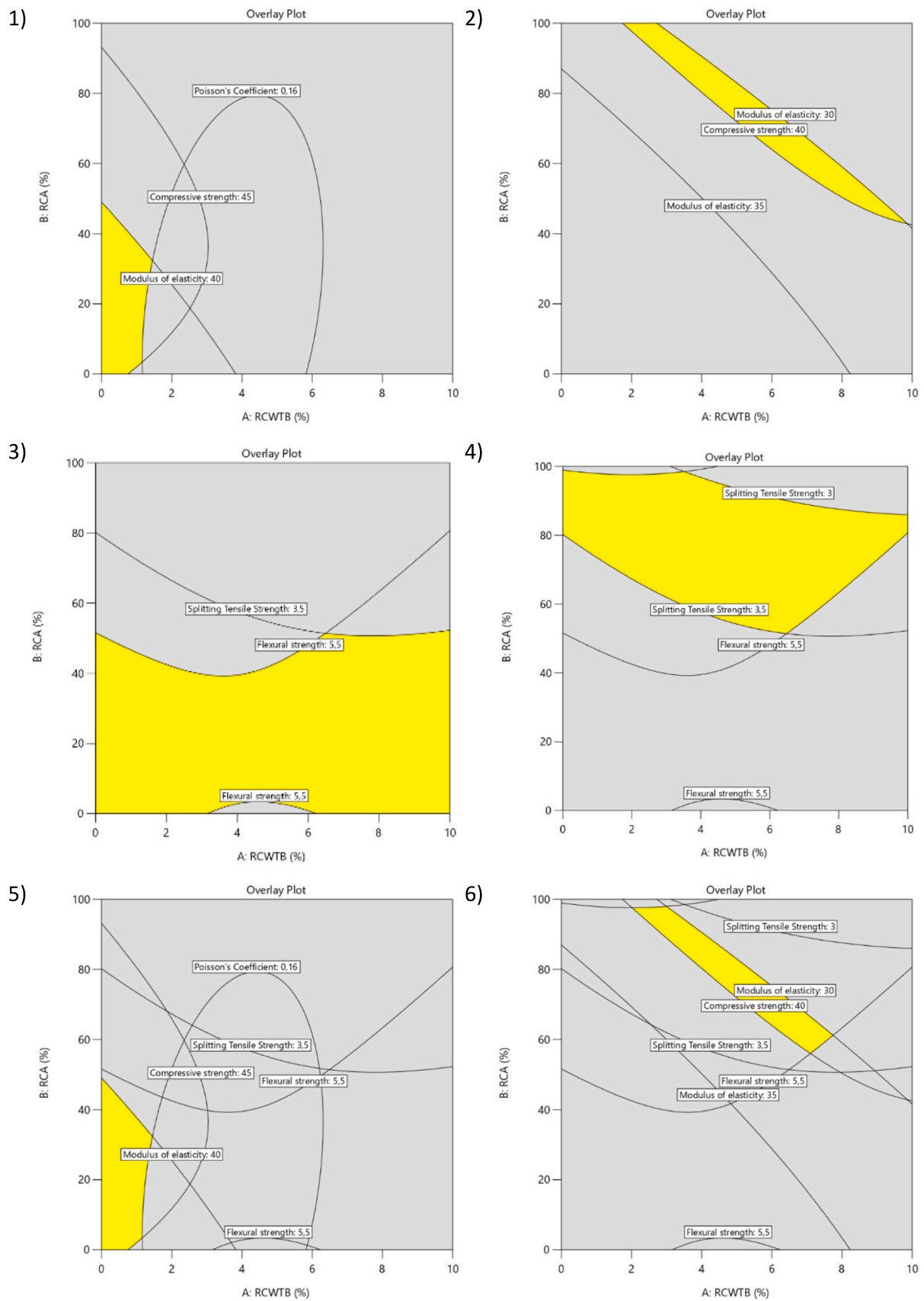


Fig. 10. Overlay plots for the case studies representing the optimal regions for combination of both residues.

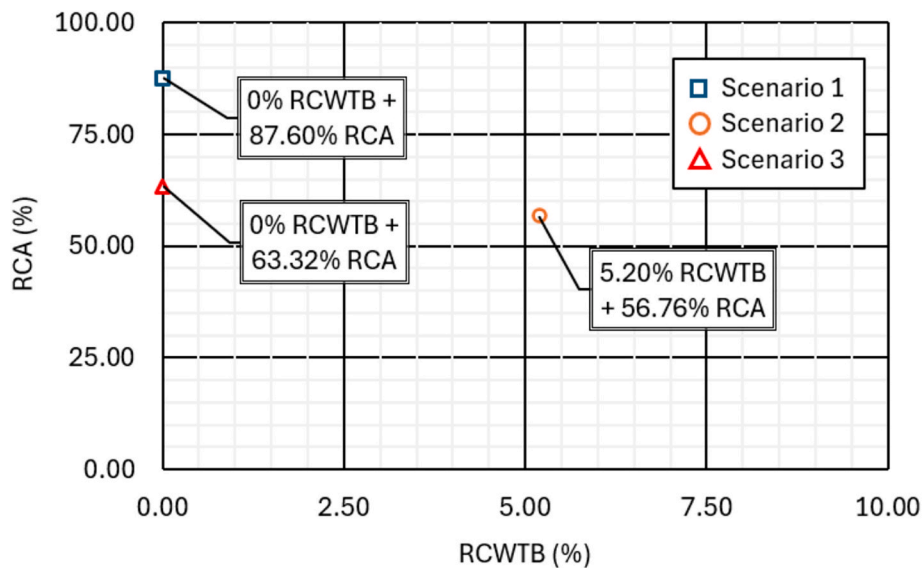


Fig. 11. Numerical optimization solutions for different scenarios evaluated.

simultaneously. Minor deviations in RCWTB and RCA proportions quickly led to one or both properties falling outside their desired ranges, further highlighting the sensitivity of performance to mix proportions.

Beyond the optimal region, approximately defined as 2–10% RCWTB and 40–100% RCA, adjustments often improved one property at the expense of the other. For instance, along the modulus of elasticity contour, compressive strength frequently failed to meet the 40 MPa target unless the proportions aligned precisely with the narrow optimal region. The close proximity of contour lines indicates steep performance gradients, emphasizing the delicate balance required in mix design. This highlights the critical challenge of achieving both high compressive strength and a desirable modulus of elasticity simultaneously, as explained in the previous case study.

5.1.3. Case study 3

In this scenario, two properties characterizing the flexural and tensile behavior of concrete were optimized. The resulting contour lines, illustrated in Fig. 10.3, intersected, revealing an interaction between the two properties that enables a relatively straightforward adjustment of the RCWTB and RCA proportions to achieve both targets simultaneously. Unlike the previous cases, the optimal region was considerably larger and ranked the highest among all evaluated cases, indicating greater flexibility in meeting the desired values for both properties concurrently. The optimal region was defined within the range of 0–10% RCWTB and 0–50% RCA.

In the upper portion of the graph, the contour associated with indirect tensile strength (3.5 MPa) approaches the upper boundary of the optimal region. This suggests that in this area, the selected proportions of both recycled materials allow the splitting tensile strength target to be reached, though the flexural strength objective may remain unmet. The transition between the optimal region and non-compliance areas is gradual, highlighting a reduced sensitivity of these properties to minor fluctuations in the proportions of recycled components.

This behavior underscores a more complementary relationship between flexural and tensile strength, facilitating their simultaneous optimization with minimal trade-offs or conflicts. The findings suggest that these mechanical properties exhibit a synergistic interaction, making the optimization process not only achievable but also practical for implementation. Nevertheless, the high implicit experimental variability has also to be accounted for, despite the large area of requirement fulfillment in terms of bending performance.

5.1.4. Case study 4

As in the previous case, the optimal region exhibits a considerable size and is primarily located in the upper section of the graph (Fig. 10.4). This positioning indicates that both properties can be optimized with high contents of recycled materials, specifically within the range of 0–10% RCWTB and 50–100% RCA. Furthermore, the extension of the yellow-shaded region spans the entire RCWTB axis, suggesting that this material plays a crucial role in optimizing the flexural and tensile properties.

In the lower section of the graph, the flexural strength target of 4.5 MPa was achieved, although the splitting tensile strength remained outside the desired range. This pattern highlights a clear trade-off between the two properties, necessitating precise adjustments in the mixture proportions to achieve balance. The overlapping and complementary nature of the contour curves aligns with the mechanical behavior of concrete, enabling a more adaptable optimization strategy within the widest feasible region.

5.1.5. Case study 5

Optimizing five properties under an alpha value of ± 1 revealed significant interactions between mechanical properties (Fig. 10.5), such as compressive strength and modulus of elasticity, and deformability-related properties, such as Poisson's coefficient. The resulting optimal region was exceptionally small, underscoring the difficulty of balancing all properties simultaneously, mainly conditioned by the compression-related ones. This high sensitivity to RCWTB and RCA proportions was evident in the contour curves, which indicated that optimizing one property often compromised others.

For instance, prioritizing a modulus of elasticity of 40 GPa implicitly achieved the target splitting tensile and flexural strength. However, meeting the flexural strength target (5.5 MPa) often compromised Poisson's coefficient requirements. The narrow optimal region highlights the necessity of prioritizing certain properties based on structural or functional requirements. Balancing five competing properties remains a complex challenge, underscoring the importance of customized optimization strategies.

5.1.6. Case study 6

The final case (Fig. 10.6), modeled with an alpha value of ± 1 , also revealed a narrow and elongated optimal region. For properties such as modulus of elasticity and compressive strength, the optimal region was located near the intersection of their respective contours, suggesting a

favorable relationship. However, this relationship also constrained the simultaneous achievement of desired values for other properties.

Attaining both a high modulus of elasticity and strong flexural-tensile performance required rigorous control over RCWTB and RCA proportions. The contour curves revealed that for many combinations, at least one property fell outside the target range. As in Case Study 5, successful optimization required prioritization of specific properties based on their structural or functional relevance, as achieving all objectives concurrently proved extremely challenging.

5.2. Numerical optimization

Following the graphical optimization process, which resulted in the generation of various 2D plots, numerical optimization was conducted using the Design Expert software, in accordance with the three scenarios outlined in Section 2.6. Fig. 11 presents the graphical representation of both waste materials for the three studied scenarios. This optimization provided precise proportions of both materials that met the predefined objectives.

As illustrated in Fig. 11, Scenario 1 focused on maximizing compressive strength and elastic modulus while maintaining Poisson's coefficient within acceptable ranges. The resulting optimal combination comprised 0% RCWTB and 87.60% RCA. Conversely, Scenario 2 aimed to optimize flexural and tensile strength properties. This led to an optimal combination of 56.76% RCA and 5.20% RCWTB, where intermediate RCA contents, combined with intermediate additions of RCWTB, contributed to developing concrete with peak flexural-tensile properties.

Finally, Scenario 3 sought to maximize compressive strength, elastic modulus, flexural strength, and splitting tensile strength while ensuring Poisson's coefficient remained within standard limits. This optimization was more complex due to the greater number of variables involved compared to the previous cases. The resulting optimal mix consisted of 0% RCWTB and 63.32% RCA. This indicated that excluding RCWTB was necessary to achieve maximum values of strength and elastic stiffness in compression terms, as its inclusion adversely impacted the mix despite the reduction in GWP and cost it caused. Meanwhile, flexural-tensile properties maintained suitable and even improved values when adding this waste.

In conclusion, the optimization outcomes for all three cases suggest that RCWTB is the dominant variable in optimal design. This highlights the significant influence of RCWTB on the mechanical and deformability properties of concrete evaluated during optimization. The negligible incorporation of RCWTB in the optimal configuration in Scenario 1 and Scenario 3 may suggest limitations in its beneficial effects in terms of compression performance. This waste may be especially recommendable when the objective is to optimize properties related to flexural behavior, as depicted through Scenario 2.

6. Conclusions

This research investigated the optimization of concrete mixes incorporating Raw-Crushed Wind-Turbine Blade (RCWTB) and coarse Recycled Concrete Aggregate (RCA) using Response Surface Methodology (RSM). Both materials were recovered from dismantled wind farms and were incorporated into concrete mixtures with proportions ranging from 0–10% RCWTB and 0–100% RCA, replacing NA. The water and admixture contents were increased when adding both wastes, in order to compensate for the expected loss of workability resulting from their addition to concrete. The study evaluated the mechanical properties of the resulting concrete mixtures, their environmental impact, and the economic cost of their production. Several models were then developed to identify the optimal combinations of RCWTB and RCA for specific applications. The main findings of this study are summarized below.

- The addition of RCWTB and RCA reduced compressive strength and stiffness of concrete, due to their deformable nature. However, maximum RCWTB additions (10%) combined with moderate RCA contents (50%) were effective in optimizing flexural and tensile properties, as the fibers in RCWTB improved crack resistance and flexural performance.
- Simultaneous additions of RCWTB and RCA also led in general to reductions in GWP and cost compared to the reference mix. The addition of any RCA content consistently reduced both properties. However, the incorporation of high RCWTB amounts occasionally increased GWP and final costs compared to concrete mixes with lower RCWTB proportions, because of the adjustments in water and admixture contents needed to maintain proper workability.
- Quadratic RSM models outperformed linear models, regardless of the alpha value used. Specifically, an alpha value of ± 1 provided the best fit for compressive strength, modulus of elasticity, and Poisson's coefficient. Conversely, an alpha value of ± 0.5 was more suitable for flexural strength, splitting tensile strength, GWP, and cost, as these properties exhibited lower curvatures and steeper gradients along their respective response surfaces.
- The response surface analysis revealed that RCWTB had a stronger influence on flexural-tensile properties, while RCA had variable effects on mechanical properties, with moderate contents usually yielding optimal results. For GWP and production cost, the impact of both wastes had a more linear nature.
- Regarding the multi-objective graphical optimization, the resulting regions were highly compact when prioritizing compression-related properties, underscoring the sensitivity of these properties to mix proportions. For flexural-tensile optimization, the optimal regions were considerably larger, with proportions of both waste materials ranging from 0–10% for RCWTB and 0–100% for RCA, indicating that flexural and tensile properties exhibited synergistic behavior. Optimizing all properties simultaneously was mainly conditioned by the compression-related ones.
- The numerical optimization results highlighted specific optimal combinations of the two materials. For instance, 0% RCWTB and 88% RCA maximized compressive strength and modulus of elasticity while keeping the Poisson's coefficient within acceptable limits. Intermediate proportions, such as 5.2% RCWTB and 56% RCA, maximized both flexural strength and splitting tensile strength, confirming the synergistic effect of these materials in enhancing flexural-tensile properties.

It is concluded that the optimization of concrete mixes incorporating RCWTB and RCA using the RSM provided valuable insights into the behavior of these recycled materials, not only in terms of their influence on the mechanical properties of concrete but also from economic and environmental perspectives. Striking a balance between RCWTB additions and RCA usage has the potential to enhance the strength of concrete.

7. Limitations and future research directions

The research presented in this article was conducted with RCWTB obtained from a single type of wind turbine blade, with a concrete design based on increasing the proportions of water and admixtures to maintain workability when adding both wastes, and focusing exclusively on the 28-day mechanical properties. Therefore, the following lines of research could be considered for future studies:

- Further investigate the mechanical behavior at later ages and the long-term durability (such as freeze–thaw resistance and carbonation, among others) of concrete produced with the optimal contents of RCA and RCWTB yielded in this study. Also, evaluate the interaction mechanism and interfacial bonding between these waste materials and the cementitious matrix of concrete for such waste

contents through micro-structural analyses such as scanning electron microscopy.

- Estimate the GWP and cost of concrete mixtures with optimal RCA and RCWTB contents, including the full environmental impacts and generalized costs of the production of these wastes in the analysis.
- Analyze the characteristics and composition of RCWTB obtained from other types of wind turbine blades and its impact on concrete behavior.
- Evaluate the effects of coarse RCA and RCWTB on concrete using a mix design in which the addition of both residues does not result in an increase in water and admixture content.

CRediT authorship contribution statement

Nerea Hurtado-Alonso: Writing – original draft, Validation, Software, Methodology, Investigation, Formal analysis, Conceptualization. **Javier Manso-Morato:** Writing – review & editing, Visualization, Validation, Software, Methodology, Investigation, Formal analysis, Conceptualization. **Víctor Revilla-Cuesta:** Writing – review & editing, Visualization, Validation, Software, Methodology, Investigation, Formal analysis. **Vanesa Ortega-López:** Writing – review & editing, Supervision, Resources, Project administration, Methodology, Funding acquisition, Conceptualization. **Marta Skaf:** Writing – review & editing, Supervision, Resources, Project administration, Methodology, Funding acquisition, Conceptualization.

Declaration of competing interest

The authors declare that they have no known competing financial interests or personal relationships that could have appeared to influence the work reported in this paper.

Data availability

Data will be made available on request.

References

- Ahmed, W., Lim, C.W., 2021. Production of sustainable and structural fiber reinforced recycled aggregate concrete with improved fracture properties: A review. *J. Clean. Prod.* 279, 123832. <https://doi.org/10.1016/j.jclepro.2020.123832>.
- Alqadi, A.N.S., Bin Mustapha, K.N., Naganathan, S., Al-Kadi, Q.N.S., 2012. Uses of central composite design and surface response to evaluate the influence of constituent materials on fresh and hardened properties of self-compacting concrete. *KSCCE J Civ Engin* 16, 407–416. <https://doi.org/10.1007/s12205-012-1308-z>.
- Ecoinvent Centre, Ecoinvent database, (2023). <https://ecoinvent.org/the-ecoinvent-database/> (accessed October 31, 2023).
- Chau, C.K., Leung, T.M., Ng, W.Y., 2015. A review on Life Cycle Assessment, Life Cycle Energy Assessment and Life Cycle Carbon Emissions Assessment on buildings. *Appl. Energy* 143, 395–413. <https://doi.org/10.1016/j.apenergy.2015.01.023>.
- Chelladurai, S.J.S., Murugan, K., Ray, A.P., Upadhyaya, M., Narasimharaj, V., Gnanasekaran, S., 2021. Optimization of process parameters using response surface methodology: A review. *Mater. Today Proc.* 37, 1301–1304. <https://doi.org/10.1016/j.matpr.2020.06.466>.
- CML - Department of Industrial Ecology, CML-IA characterization factors (2016). <https://www.universiteitleiden.nl/en/research/research-output/science/cml-ia-characterisation-factors> (accessed October 30, 2023).
- Structural Code, Código Estructural de España, Spanish Structural Code, Ministerio de Fomento, Gobierno de España (2021).
- Da Silva, A., Kyriakides, S., 2007. Compressive response and failure of balsa wood. *Int. J. Solids Struct.* 44, 8685–8717. <https://doi.org/10.1016/j.ijstr.2007.07.003>.
- De, B., Bera, M., Bhattacharjee, D., Ray, B.C., Mukherjee, S., 2024. A comprehensive review on fiber-reinforced polymer composites: Raw materials to applications, recycling, and waste management. *Prog Mater Sci* 146, 101326. <https://doi.org/10.1016/j.pmatsci.2024.101326>.
- Devènes, J., Bastien-Masse, M., Widmer, N., Fivet, C., 2023. Low-tech methods for the reuse of reinforced concrete structural elements. *J. Phys. Conf. Ser.* 2600, 192005. <https://doi.org/10.1088/1742-6596/2600/19/192005>.
- Djerbi Tegguer, A., 2012. Determining the water absorption of recycled aggregates utilizing hydrostatic weighing approach. *Constr. Build. Mater.* 27, 112–116. <https://doi.org/10.1016/j.conbuildmat.2011.08.018>.
- EN-Euronorm, EN-Euronorm. Rue de stassart, 36. Belgium-1050 Brussels, European Committee for Standardization (2020).
- Eurocode 2, Eurocode 2, Design of Concrete Structures. Part 1-1: General Rules and Rules for Buildings (EN 1992-1-1). CEN (European Committee for Standardization), 2010.
- Evangelista, L., de Brito, J., 2010. Durability performance of concrete made with fine recycled concrete aggregates. *Cem. Concr. Compos.* 32, 9–14. <https://doi.org/10.1016/j.cemconcomp.2009.09.005>.
- Fenner, A.E., Kibert, C.J., Woo, J., Morque, S., Razkenari, M., Hakim, H., Lu, X., 2018. The carbon footprint of buildings: A review of methodologies and applications. *Renew. Sustain. Energy Rev.* 94, 1142–1152. <https://doi.org/10.1016/j.rser.2018.07.012>.
- Fort, J., Cerný, R., 2020. Transition to circular economy in the construction industry: Environmental aspects of waste brick recycling scenarios. *Waste Manag.* 118, 510–520. <https://doi.org/10.1016/j.wasman.2020.09.004>.
- Government of Extremadura, Construction Prices Guide (Spanish) (2024). <http://basepreciosconstruccion.gobex.es/>.
- Habert, G., Miller, S.A., John, V.M., Provis, J.L., Favier, A., Horvath, A., Scrivener, K.L., 2020. Environmental impacts and decarbonization strategies in the cement and concrete industries. *Nat. Rev. Earth Environ.* 1, 559–573. <https://doi.org/10.1038/s43017-020-0093-3>.
- Haider, M.M., Nassiri, S., Englund, K., Li, H., Chen, Z., 2021. Exploratory study of flexural performance of mechanically recycled glass fiber reinforced polymer shreds as reinforcement in cement mortar, in: *Transp Res Rec*, SAGE Publications Ltd 1254–1267. <https://doi.org/10.1177/03611981211015246>.
- Honic, M., Kovacic, I., Aschenbrenner, P., Ragossnig, A., 2021. Material Passports for the end-of-life stage of buildings: Challenges and potentials. *J. Clean. Prod.* 319, 128702. <https://doi.org/10.1016/j.jclepro.2021.128702>.
- Hossain, M.A., Ayodele, B.V., Cheng, C.K., Khan, M.R., 2019. Optimization of renewable hydrogen-rich syngas production from catalytic reforming of greenhouse gases (CH₄ and CO₂) over calcium iron oxide supported nickel catalyst. *J En Inst* 92, 177–194. <https://doi.org/10.1016/j.joei.2017.10.010>.
- Hurtado-Alonso, N., Manso-Morato, J., Revilla-Cuesta, V., Skaf, M., Ortega-López, V., 2024. Optimization of cementitious mixes through response surface method: a systematic review. *Arch. Civ. Mech. Eng.* 25, 54. <https://doi.org/10.1007/s43452-024-01112-3>.
- Islam, M.J., Shahjalal, M., Haque, N.M.A., 2022. Mechanical and durability properties of concrete with recycled polypropylene waste plastic as a partial replacement of coarse aggregate. *J Build Eng* 54, 104597. <https://doi.org/10.1016/j.jobe.2022.104597>.
- Joustra, J., Flipsen, B., Balkenende, R., 2021. Structural reuse of wind turbine blades through segmentation. *Comp Part c: Open Access* 5, 100137. <https://doi.org/10.1016/j.jcomc.2021.100137>.
- Kurda, R., Silvestre, J.D., de Brito, J., 2018. Life cycle assessment of concrete made with high volume of recycled concrete aggregates and fly ash. *Resour. Conserv. Recycl.* 139, 407–417. <https://doi.org/10.1016/j.resconrec.2018.07.004>.
- Li, S., Qin, X., Zhang, G., Xu, Y., Lv, Y., 2020. Optimization of content of components over activated carbon catalyst on CO₂ reforming of methane using multi-response surface methodology. *Int J Hydrog Energy* 45, 9695–9709. <https://doi.org/10.1016/j.ijhydene.2020.01.226>.
- Li, L., Wang, L., Zhang, X., 2022. Technology Innovation for Sustainability in the Building Construction Industry: An Analysis of Patents from the Yangtze River Delta, China. *Buildings* 12 (12), 2205. <https://doi.org/10.3390/buildings12122205>.
- Liu, P., Barlow, C.Y., 2017. Wind turbine blade waste in 2050. *Waste Manag.* 62, 229–240. <https://doi.org/10.1016/j.wasman.2017.02.007>.
- Liu, T., Paraskevoulakos, C., Mughal, U.A., Tyurkay, A., Lushnikova, N., Song, H., Duyal, C., Karnick, S.T., Gauvin, F., Lima, A.T., 2025. Mechanisms and applications of wind turbine blade waste in cementitious composites: A review. *Mater. Des.* 251, 113732. <https://doi.org/10.1016/j.matdes.2025.113732>.
- Luhar, S., Luhar, I., 2019. Potential application of E-wastes in construction industry: A review. *Constr Build Mater* 203, 222–240. <https://doi.org/10.1016/j.conbuildmat.2019.01.080>.
- Memon, S., Bekzhanova, Z., Murzakarimova, A., 2022. A Review of Improvement of Interfacial Transition Zone and Adherent Mortar in Recycled Concrete Aggregate. *Buildings* 12 (19), 1600. <https://doi.org/10.3390/buildings12101600>.
- S.P. Muñoz Pérez, J.M. Pardo Becerra, J.M. García Chumacero, E. Sánchez Diaz, E.A. Diaz Ortiz, E.D.R. Laffite, J.L. Quispe Osorio, Y.M. Briceno Mendoza, Evaluation of the physical and mechanical properties of concrete with the incorporation of recycled concrete aggregate, *Inn Infr Sol* 9 (2024) 204. doi: 10.1007/s41062-024-01517-2.
- Muresan, A., Brütting, J., Redaelli, D., Fivet, C., 2020. Sustainability through reuse: a reconfigurable structural system for residential and office buildings. *IOP Conf. Ser.: Earth Environ. Sci* 588, 042066. <https://doi.org/10.1088/1755-1315/588/4/042066>.
- F. Nygaard Rasmussen, H. Birgisdottir, Life cycle environmental impacts from refurbishment projects – a case study, 2016.
- Omojola, A., Kallon, D., Bello, K., 2022. Resource Recycling with the Aim of Achieving Zero-Waste Manufacturing. *Sustainability* 14 (8), 4503. <https://doi.org/10.3390/su14084503>.
- Padmini, A.K., Ramamurthy, K., Mathews, M.S., 2009. Influence of parent concrete on the properties of recycled aggregate concrete. *Constr. Build. Mater.* 23, 829–836. <https://doi.org/10.1016/j.conbuildmat.2008.03.006>.
- Pedro, D., de Brito, J., Evangelista, L., 2017. Structural concrete with simultaneous incorporation of fine and coarse recycled concrete aggregates: Mechanical, durability and long-term properties. *Constr. Build. Mater.* 154, 294–309. <https://doi.org/10.1016/j.conbuildmat.2017.07.215>.
- Poorisat, T., Aigwi, I.E., Doan, D.T., GhaffarianHoseini, A., 2024. Unlocking the potentials of sustainable building designs and practices: A Systematic Review. *Build. Environ.* 266, 112069. <https://doi.org/10.1016/j.buildenv.2024.112069>.

- Rambabu, D., Sharma, S.K., Abdul Akbar, M., 2022. A review on suitability of using geopolymer concrete for rigid pavement. *Inn Infr Sol* 7 286. <https://doi.org/10.1007/s41062-022-00878-w>.
- Revilla-Cuesta, V., Skaf, M., Ortega-López, V., Manso, J.M., 2023. Raw-crushed wind-turbine blade: Waste characterization and suitability for use in concrete production. *Resour. Conserv. Recycl.* 198, 107160. <https://doi.org/10.1016/j.resconrec.2023.107160>.
- Revilla-Cuesta, V., Hurtado-Alonso, N., Manso-Morato, J., Serrano-López, R., Manso, J. M., 2024. Effects of temperature and moisture fluctuations for suitable use of raw-crushed wind-turbine blade in concrete. *Environ Sci Poll Res* 31, 37757–37776. <https://doi.org/10.1007/s11356-024-33720-0>.
- Revilla-Cuesta, V., Manso-Morato, J., Hurtado-Alonso, N., Skaf, M., Ortega-López, V., 2024. Mechanical and environmental advantages of the revaluation of raw-crushed wind-turbine blades as a concrete component. *J Build Eng* 82, 108383. <https://doi.org/10.1016/j.jobe.2023.108383>.
- Database and Support Teams at PRÉ Sustainability, SimaPro 9.5. What's new?, 2023.
- Spini, F., Bettini, P., 2024. End-of-Life wind turbine blades: Review on recycling strategies. *Compos. B Eng.* 275, 111290. <https://doi.org/10.1016/j.compositesb.2024.111290>.
- Tahir, H., Khan, M., Shafiq, N., Radu, D., Hadzima-Nyarko, M., Waqar, A., Almujiabah, H., Benjeddou, O., 2023. Optimisation of Mechanical Characteristics of Alkali-Resistant Glass Fibre Concrete towards Sustainable Construction. *Sustainability* 15 (14), 11147. <https://doi.org/10.3390/su151411147>.
- Tekle, B., Holschemacher, K., Löber, P., Heiden, B., 2021. Mechanical Behavior and Frost-Resistance of Alkali-Activated Cement Concrete with Blended Binder at Ambient Curing Condition. *Buildings* 11 (2), 52. <https://doi.org/10.3390/buildings11020052>.
- Ulucan, M., 2024. From waste to sustainable production: Experimental design and optimization of sustainable concrete using response surface methodology and life cycle assessment. *Sustain. Chem. Pharm.* 42, 101770. <https://doi.org/10.1016/j.scp.2024.101770>.
- M. xin Xu, H. wen Ji, Y. chang Wu, X. xi Meng, J. yi Di, J. Yang, Q. Lu, Recovering glass fibers from waste wind turbine blades: Recycling methods, fiber properties, and potential utilization, *Renew Sustain Energy Rev* 202 (2024) 114690. doi: 10.1016/j.rser.2024.114690.
- Xu, G.T., Liu, M.J., Xiang, Y., Fu, B., 2022. Valorization of macro fibers recycled from decommissioned turbine blades as discrete reinforcement in concrete. *J. Clean. Prod.* 379, 134550. <https://doi.org/10.1016/j.jclepro.2022.134550>.
- Yao, X., Pei, Z., Zheng, H., Guan, Q., Wang, F., Wang, S., Ji, Y., 2022. Review of Mechanical and Temperature Properties of Fiber Reinforced Recycled Aggregate Concrete. *Buildings* 12 (8), 1224. <https://doi.org/10.3390/buildings12081224>.
- Zhang, B., Zhang, S., Yang, Z., Liu, W., Wu, B., Huang, M., Liu, B., 2024. Pyrolysis process and products characteristics of glass fiber reinforced epoxy resin from waste wind turbine blades. *Compos. B Eng.* 287, 111803. <https://doi.org/10.1016/j.compositesb.2024.111803>.